

REVIEW ARTICLE

Cold survival in freeze-intolerant insects

The structure and function of β -helical antifreeze proteins

Steffen P. Graether and Brian D. Sykes

CIHR Group in Protein Structure and Function, Department of Biochemistry and Protein Engineering Network of Centres of Excellence, University of Alberta, Edmonton, Alberta, Canada

Antifreeze proteins (AFPs) designate a class of proteins that are able to bind to and inhibit the growth of macromolecular ice. These proteins have been characterized from a variety of organisms. Recently, the structures of AFPs from the spruce budworm (*Choristoneura fumiferana*) and the yellow mealworm (*Tenebrio molitor*) have been determined by NMR and X-ray crystallography. Despite nonhomologous sequences, both proteins were shown to consist of β -helices. We review the structures and dynamics data of these two insect AFPs to bring insight into the structure–function relationship and explore their β -helical architecture. For the spruce budworm protein, the fold is a left-handed β -helix with 15 residues per coil. The *Tenebrio molitor* protein

consists of a right-handed β -helix with 12 residues per coil. Mutagenesis and structural studies show that the insect AFPs present a highly rigid array of threonine residues and bound water molecules that can effectively mimic the ice lattice. Comparisons of the newly determined ryegrass and carrot AFP sequences have led to models suggesting that they might also consist of β -helices, and indicate that the β -helix might be used as an AFP structural motif in nonfish organisms.

Keywords: antifreeze protein; beta-helix; dynamics; ice; insect; NMR; structure; thermal hysteresis; water; X-ray crystallography.

Introduction

Several organisms are freeze-intolerant, yet are able to survive subzero temperatures by decreasing the probability of ice nucleation in their bodies. Survival strategies include the removal of water from areas that may come in contact with external ice, physical barriers such as a silk hibernaculum, the production of high levels of polyalcohols and sugars [1], and the production of antifreeze proteins (AFPs). AFPs, also known as thermal hysteresis proteins, can effectively lower the freezing point of bodily fluids, thereby preventing the formation of macroscopic ice crystals. To date, AFPs have been isolated from a number of fish [2], plants [3], bacteria [4], fungi [5] and arthropods [6]. The proteins are thought to function by inhibiting the growth of small ice crystals [7], or by masking sites that could act as heterogeneous ice nucleators [8]. The inhibition of ice growth

is believed to occur by the Kelvin effect: the binding of AFP causes the ice between the bound proteins to grow as a curved front, where further growth becomes energetically unfavourable [7]. In this process, the freezing point of the solution is lowered whereas the melting point remains unaffected. The difference between the lowest temperature at which AFPs are able to prevent ice growth and the melting point of the solution is termed thermal hysteresis (TH), and is used as a measurement of antifreeze activity.

A large number of biochemical and structural studies have been performed in order to understand the interaction between antifreeze protein and ice at the atomic level and has included the determination of a number of fish AFP structures (Fig. 1) (reviews in [9–16]). Early models of the interaction between this class of proteins and ice focused on winter flounder type I AFP as the archetypal antifreeze protein structure. The protein is completely α -helical, and contains four Thr residues spaced 11 residues apart on one side of the helix [17,18]. Analysis of its structure and ice-binding properties led to the hypothesis that the protein binds to a specific plane of ice through hydrogen bonds from the threonyl hydroxyl groups [17,19–21]. Further experimentation, however, has questioned the relative importance of hydrogen bonds. Mutagenesis of the two central Thr residues (Thr13 and Thr24)→Ser, which would preserve the ability of the side-chain to hydrogen bond to ice, caused a 90–100% loss in TH activity (where activities are generally measured at a protein concentration of 1 mg·mL⁻¹, and mutant activities are expressed as a percentage of wild-type activity) [22–24]. In contrast, mutation of these Thr to the isosteric equivalent Val resulted in only a moderate loss (85% of wild-type activity)

Correspondence to S. P. Graether, Department of Biochemistry, University of Alberta, Edmonton, Alberta, Canada, T6G 2H7.
Fax: +780 492 0886, Tel.: +780 492 3006,
E-mail: steffen@biochem.ualberta.ca

Abbreviations: AFP, antifreeze protein; CfAFP, *Choristoneura fumiferana* antifreeze protein; DAFP, *Dendroides canadensis* antifreeze protein; DcAFP, *Daucus carota* antifreeze protein; INP, ice-nucleation protein; LpxA, UDP-*N*-acetylglucosamine 3-*O*-acyltransferase; pelC, pectate lyase C; sbwAFP, spruce budworm antifreeze protein; TH, thermal hysteresis; TmAFP, *Tenebrio molitor* antifreeze protein; TXT, Thr-X-Thr motif.

Note: A website is available at <http://www.pence.ca/~steffen>

(Received 10 May 2004, revised 15 June 2004, accepted 17 June 2004)

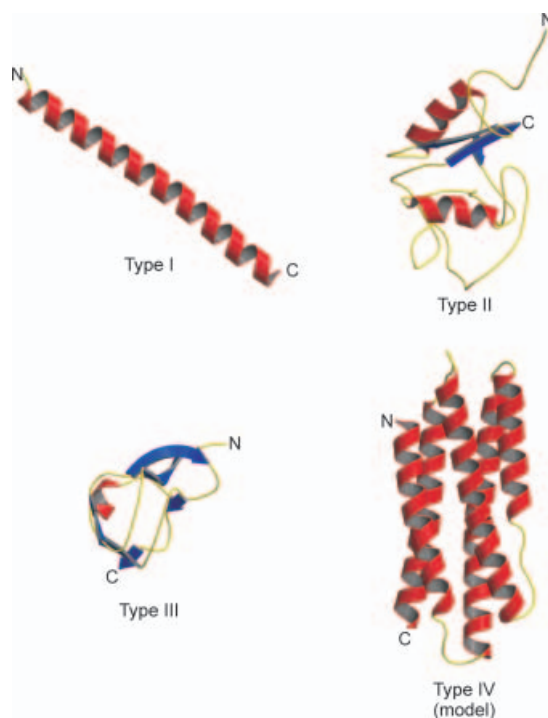


Fig. 1. Fish AFP structures and model. The structures of the fish AFPs are shown as ribbon diagrams with coil structure shown as yellow, α -helices as red and β -strands as blue. The model of type IV AFP is based on the sequence similarity to apolipoprotein III [71].

[22–24]. These results weaken the hypothesis that the Thr face of the α -helix is critical to the ice-binding interaction. Furthermore, mutation of Ala17→Leu, a residue adjacent to the Thr-rich face, abolished all antifreeze activity [25]. The ice-binding face of type I AFP is now thought to consist of the alanine-rich face (which includes Ala17) and the γ -methyls of the four threonines (Thr2, Thr13, Thr24 and Thr35) [25].

Additional structural studies have been performed on the type II AFP from sea raven [26], and on the type III AFP from eel pout [27–30]. Neither protein shows any sequence homology to each other or to type I AFP. Likewise, the structures do not show any similarity to the α -helical type I AFP (Fig. 1). For type II AFP, the fold was shown to be homologous to the C-type lectins [26]. The type III AFP structure was shown to be a compact fold of several short β -sheets, and does not possess any known structural homology [27–30]. For both of these antifreeze proteins, the structures do not reveal any repetitive arrangement of polar groups that could bind ice. The inability of researchers to propose a consistent model explaining the type III AFP/ice-binding in terms of hydrogen bonding has led to the proposal of models where ‘flatness’ [29] or ‘shape complementarity’ [12] drives binding, such that van der Waals forces dominate the interaction. This hypothesis requires considerable further refinement, as it is at the moment unable to explain the specificity of antifreeze proteins for particular planes of ice [20], or how these proteins can compete for the ice face when there is a vast excess of water that can readily hydrogen bond to ice [27].

The cloning and expression of insect AFPs from the spruce budworm (*Choristoneura fumiferana*) [31], yellow mealworm (*Tenebrio molitor*) [32] and fire-colored beetle (*Dendroides canadensis*) [33] has generated interest in a potentially new class of structures and a different model system for the study of the AFP–ice interaction. The properties of insect AFPs are remarkable in that their activities must protect against freezing temperatures that are considerably colder than that necessary for fish survival (−1.9 °C in seawater vs. −20 °C or colder for terrestrial insects). This difference was demonstrated by comparison of the activity of fish type III AFP (TH of 0.27 °C at 400 μ M) vs. spruce budworm antifreeze protein (sbwAFP) (TH of 1.08 °C at 20 μ M) [34]. The ‘hyperactivity’ of the insect AFP results in 10–100 \times greater activity on a molar basis than that produced by fish antifreeze proteins. One explanation for the greater activity has come from ice-etching experiments [20], which determine which particular planes of ice an AFP can bind at low protein concentrations. Fish AFPs have been reproducibly shown to bind to one plane, though recent studies suggest that they may be able to bind additional planes at higher concentrations [35]. Experiments using sbwAFP showed that it could bind to both prism and basal planes of ice at low protein concentrations [34]. The ability of sbwAFP to provide more effective coverage of the ice surface than fish AFPs may partly explain the greater activity of insect AFPs compared to those from other species.

To better understand the biophysical basis of this greater activity, the spruce budworm antifreeze protein (sbwAFP, also known as CfAFP) and *Tenebrio molitor* antifreeze protein (TmAfP) were cloned [31,32,36] and their three-dimensional structures were determined [34,37–40]. In subsequent sections, we describe the structure and dynamics of each protein, and present a comparison of sbwAFP and TmAfP with each other and with proteins that have a similar fold.

Structure of sbwAFP and TmAfP

The structure of sbwAFP has been determined by X-ray crystallography to 2.5 Å and by NMR at both 30 °C and 5 °C [34,37,38]. Both techniques show that the fold is a left-handed, parallel β -helix of 15 residues per coil (Fig. 2A). The shape is approximately that of a triangular prism, with each face being 17 \times 23 Å, with a total solvent accessible surface area of about 1355 Å². The three sides of the prism contain parallel β -sheets, where each individual sheet is made of four β -strands that are very flat. A cross-section containing one coil of the β -helix is shown in Fig. 2B. The Gly-Val sequence at residues 72–73 is conserved in almost all sbwAFP isoforms, and is located at the point where the coil changes from left- to right-handed. This sequence, combined with the disulphide bonds Cys67–Cys80, may be responsible for the change in handedness of the C-terminal cap [41]. The protein contains a total of four disulphide bonds located between coils. The addition of dithiothreitol, which reduces disulphide bonds, destroys the TH activity of sbwAFP [42]. The structure shows that there is a right-handed cap at the C-terminus of the protein, which forms two antiparallel sheets with β -strands from the preceding coil. The conformation of the cap varies somewhat between

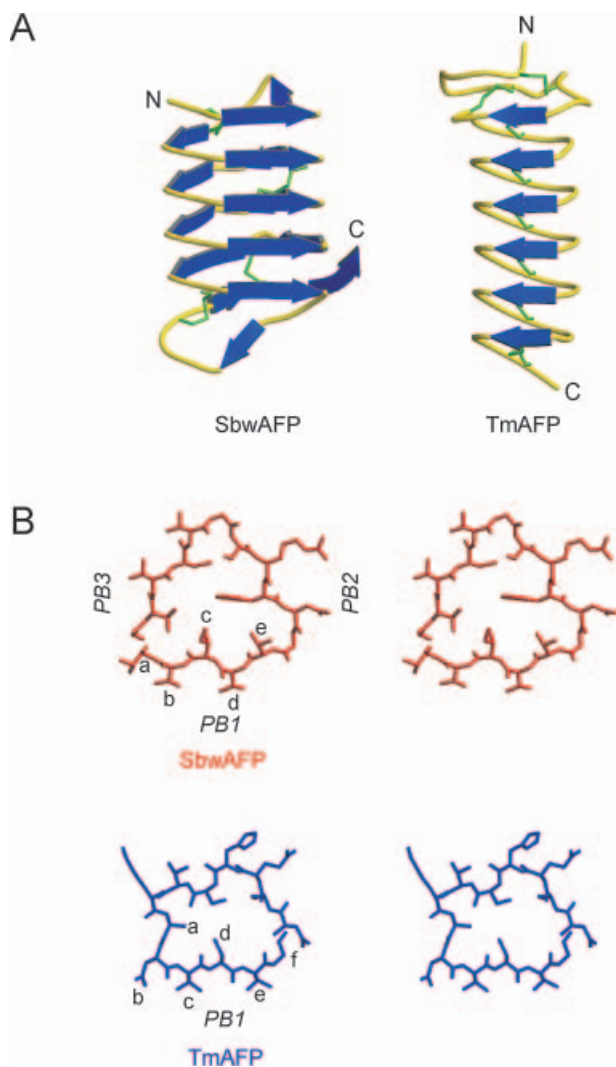


Fig. 2. Insect AFP structures. (A) A ribbon diagram of sbwAFP (PDB code 1L0S) is shown on the left, TmAFP (PDB code 1EZG) on the right. The color scheme is identical to that in Fig. 1. Disulphide bonds are displayed as green sticks. The sequence convention used for TmAFP throughout the review is based on the bacterially expressed protein starting at Met0, such that the numbering system differs from that used to describe the TmAFP crystal structure which starts at Met1 [39]. The N- and C-terminal ends of the protein are labeled N and C, respectively. (B) Stereo stick representation of one coil of sbwAFP (red, residues Gly34 to Thr49) and TmAFP (blue, residues Asn29→Gly41). Letters denote the five residues of one of the three sides of sbwAFP or six residues of one of two sides of TmAFP. The strands that make up the three, parallel β -sheets of the protein are designated PB1, PB2 or PB3 for sbwAFP. For TmAFP, there is only one face of the protein that forms a parallel β -sheet, with the strand of the coil indicated as PB1 in the figure. All figures were created using MOLSCRIPT [72] and RASTER3D [73].

the different structural methods used (Fig. 3A,B). At 5 °C (Fig. 3A), the β -strand content of this region is not as high as that seen in the X-ray and 30 °C NMR structures, suggesting that there has been a change in secondary structure as the temperature was lowered. The 30 °C NMR structure (Fig. 3B) also reveals a slightly different confor-

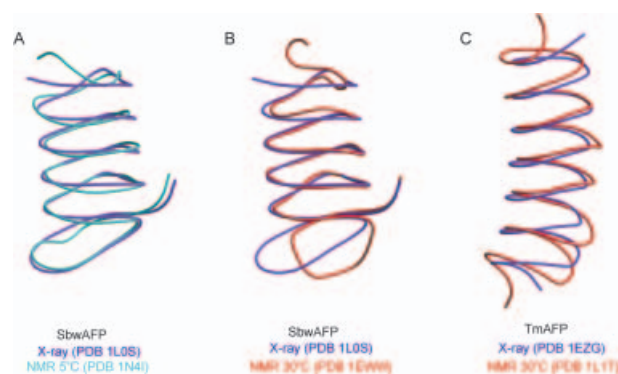


Fig. 3. Comparison of insect AFP structures solved by X-ray crystallography and NMR. The structures are shown as smoothed α traces with the method and PDB code shown below each panel. (A) Overlap of X-ray structure with 5 °C NMR structure using the main chain of residues Ser12→Thr70 in the structure alignment. (B) Overlap of the X-ray structure with the 30 °C NMR structure using the main chain of residues Ser12→Thr70 in the structure alignment. (C) Overlap of X-ray structure of TmAFP with the NMR structure determined at 30 °C using the main chain of residues Gln1→Gly80 in the structure alignment.

mation of the C-terminal cap. Rather than staying in close proximity to the previous loop, the coil at 30 °C extends further away from the previous coil compared to the X-ray and 5 °C NMR structures. One possible role for the cap structure, in conjunction with the disulphide bonds, is that it may prevent unfolding of the protein at lower temperatures. Cold denaturation, which occurs because the hydrophobic effect is weaker at lower temperatures, might result in the sbwAFP no longer being able to bind to ice because of a loss in structure.

As with the antifreeze protein from spruce budworm, both the 1.4 Å X-ray and 30 °C NMR structures of TmAFP have been determined (Fig. 2A) [39,40]. The overall shape is that of a flattened cylinder, resulting in a total solvent accessible surface area of 1180 Å² with a pseudo-rectangular face of 6.5 × 15 Å. The β -helical fold in this case consists of only one β -sheet face with six β -strands but like sbwAFP the β -strands are very flat. An overlap of the X-ray structure and 30 °C NMR structure is shown in Fig. 3C. The secondary structure assignment is similar between the two methods, although the NMR data did not show a β -strand in the final coil. The N-terminus demonstrates poor overlap between the two structures, but this is most likely due to the solution structure being loosely defined in this region [40].

The structure of TmAFP is even more regular than that of sbwAFP, and may be one of the most regular structures determined to date. In addition, each coil has a nearly identical structure, where six of the seven coils have an RMSD of 0.48 ± 0.02 Å (Fig. 2C) [39]. An exception is the N-terminal cap, which is 14 residues long and does not have the same conformation as the subsequent coils. The regularity of the structure can be attributed to the lack of a hydrophobic core typically found in globular proteins. Instead, there is a rung of disulphides down the middle of the protein. The addition of dithiothreitol destroys the TH activity [43], most likely due to complete loss of structure. Core residues also contain Ser and Ala, where the Ser

hydroxyl group is within hydrogen bonding distance to two backbone amides. A stack of internal water molecule near the Ala core residues substitutes for the Ser hydroxyl groups, as it is also able to hydrogen bond to backbone atoms.

Comparison of sbwAFP and TmAFP with other β -helical proteins

The first protein identified to have a right-handed parallel β -helical fold was pectate lyase (pelC) [44], while UDP-*N*-acetylglucosamine 3-*O*-acyltransferase (LpxA) [45] was the first protein identified to have a left-handed parallel β -helical fold. β -Helical proteins consist of coils typically 18 (left-handed) or ≈ 22 (right-handed) residues in length that wrap around the long axis of the protein. The fold name ' β -helix' arises from the helical path that the coils follow, and the β -sheets that are found on one or more faces of the protein perpendicular to the helical axis. The strands from the β -sheets are spaced 4.8 Å apart and are relatively flat and untwisted compared to β -sheets found in non β -helical proteins [41]. They also contain cupped-stacks of residues [45], which refer to the stacks of side-chains on top of one another that have similar χ_1 angles (i.e. equivalent geometric positions of the side-chain atoms rather than equivalent angles). Polar residues are rarely located in the hydrophobic core, but occasionally aromatic residues are found [41]. Small polar residues are required in order to allow for tight turns to form [45]. An unusual property of left-handed helices is that most extended polypeptides with L-amino acids have an inherent right-handed twist [46]. The left-handed β -helices have β -strands with left-handed crossover connections, which may be derived from the unusually flat β -sheets [41,47].

Parallel β -helices have been proposed to form a link between globular and fibrous proteins because of their highly repetitive structure, such that amyloid fibrils may have a parallel β -helical structure [48,49]. During freeze/thaw experiments using fish type I AFP experiments, we found that the protein formed a gel with dye-binding properties identical to that of disease-state amyloid fibrils [50]. Initially, we hypothesized that the type I AFP, which is α -helical in solution, may be forming a structure similar to that of the insect β -helical proteins when bound to ice. This hypothesis is most probably incorrect, as at lower concentrations of protein, the structure can remain α -helical (S. P. Graether, C. M. Slupsky & B. D. Sykes, unpublished observation), and given the irreversibility of the gel formation, the change in structure is unlikely to provide effective protection against *in vivo* ice growth.

The structure of the 15 residues per coil sbwAFP is very homologous to that of the 18-residue per coil of LpxA (Fig. 4A). A structural homology search using the program COMBINATORIAL EXTENSION [51] suggests that the sbwAFP fold is a match to the β -helical hexapeptide repeat proteins, despite the difference in the number of residues per coil. LpxA has a total of 10 coils plus an α -helical extension at the C-terminus, compared to the five coils of sbwAFP, making LpxA more than twice as long. The side-chain of residues on the sides of the triangular cross-section of sbwAFP follow the similar alternate in/out pattern of LpxA [where 'in' refers to a side-chain pointing into the hydrophobic core (Fig. 4B)]. An exception occurs at the corners, where in

the 18-residue per coil β -helices, the amino acids point sequentially out-out. This accommodates the 'extra' residue in the coil compared to that of the insect AFP. Another difference is that there are additional structural elements in LpxA that loop out from individual coils and act as ligand binding sites. SbwAFP, in contrast, is essentially a free-standing β -helix with a C-terminal cap. The lack of such extensions on sbwAFP suggests that the structure has been optimized for its role as an ice-binding protein rather than as an enzyme.

A recent BLAST search (April, 2004) did not reveal any sbwAFP sequence homologues other than the known isoforms. In contrast, a search using TmAFP revealed several potential matches. The top matches are to the antifreeze protein from *Dendroides canadensis* AFP (DAFP), an insect related to *Tenebrio molitor* [52]. A model of DAFP based on the structure of TmAFP has been proposed [12], and suggests that the two proteins have essentially identical structures, which is not surprising given the 40–60% sequence homology between them. Subsequent sequence matches do not make sense and most likely occur because of the high Cys content in TmAFP.

A structural homology search using TmAFP using the COMBINATORIAL EXTENSION program [51] did not reveal any matches, demonstrating the uniqueness of this fold. A comparative structural analysis cannot be made easily between TmAFP and other, right-handed β -helical proteins, because all other known right-handed β -helical proteins have coils that consist of approximately 22 residues, nearly double the 12 residues per coil of TmAFP. One of the few similarities includes a cap structure at the N-terminus of these proteins. As with sbwAFP, TmAFP has fewer coils than the other right-handed β -helical proteins (Fig. 4A), and does not have extensions from the coils that can act as ligand binding sites. An overlap of one coil of pelC and TmAFP is shown in Fig. 4B. The overlap emphasizes the similarity of the β -strand along the TXT face of TmAFP. Even though the number of residues is approximately half, the disulphide core of TmAFP and resultant tight structure give a cross-sectional area that is less than half that of the pelC protein.

Mutagenesis of insect AFPs

Analysis of the structures combined with information from isoform sequences and mutation experiments may provide clues to understanding AFP ice binding. The most notable sequence property is the conservation of Thr-X-Thr (where X can be any amino acid; abbreviated to TXT) in sbwAFP, TmAFP and the *Tenebrio molitor* related DAFP. While mutation data of type I AFP has shown that the Thr hydroxyl may not be as essential to ice-binding as first hypothesized, it is difficult not to propose that the TXT motif in the insect AFPs is relevant to the binding interaction. Structurally, the TXT motifs are clustered onto one face of sbwAFP and TmAFP (Fig. 5). Support for the importance of the TXT motif in the ice-binding interaction came from mutation studies. Mutations to a longer side-chain such as Leu or Tyr could prevent residues along the TXT face from binding to ice because of steric interference. Individual mutation of the Thr residues (Thr7→Leu, Thr21→Leu, Thr38→Leu, Thr51→Leu and Thr70→Leu)

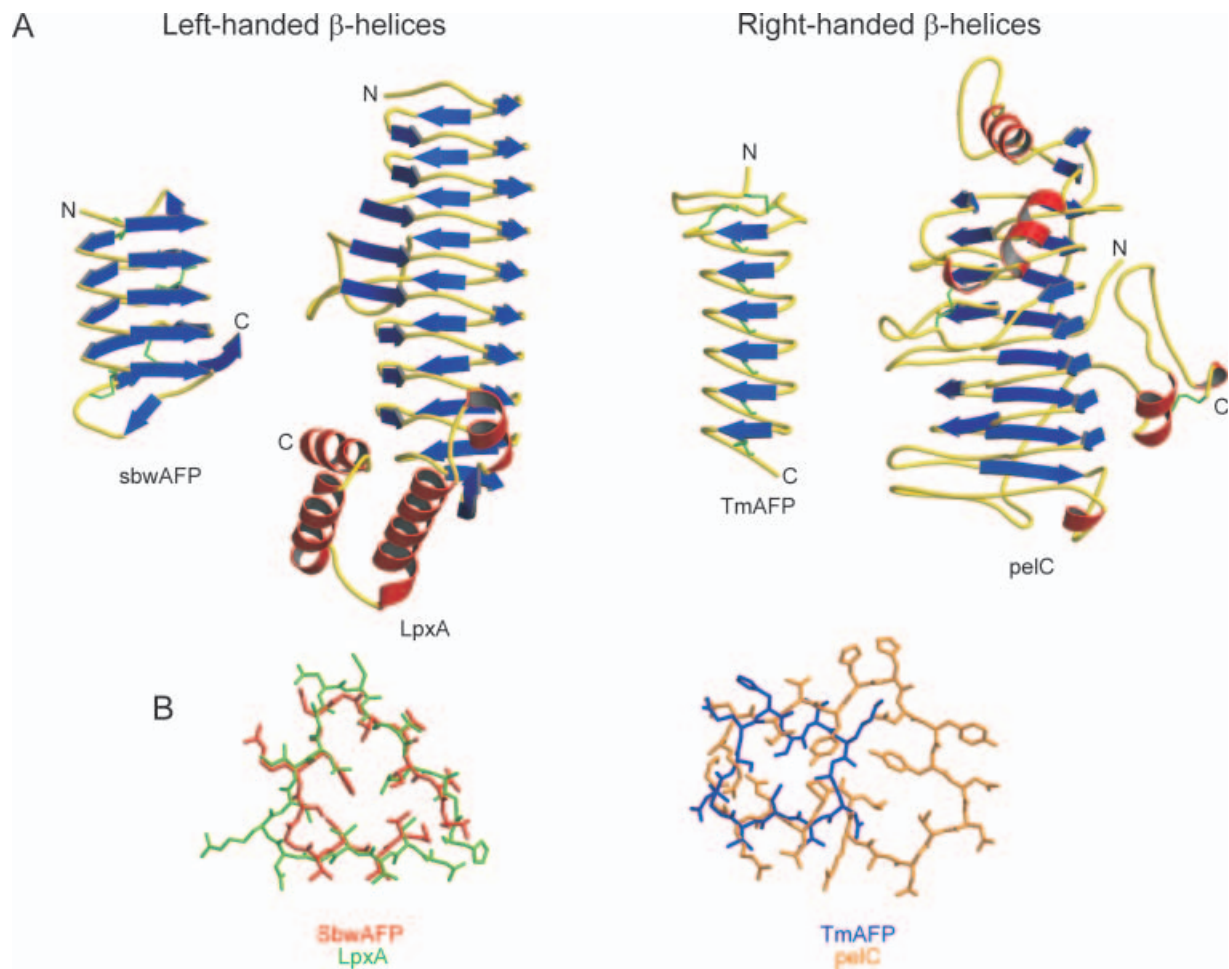


Fig. 4. Comparison of the insect β -helical structures with other β -helical proteins. (A) Ribbon representation of sbwAFP, LpxA, TmAFP and pelC. The color scheme is identical to that used in Fig. 1. Structures are oriented such that the N-termini are near the top of the panel, while the C-termini are near the bottom. (B) Overlap of individual coils of sbwAFP with LpxA and TmAFP with pelC. Proteins are colored according to the label shown below the structure, with the coils shown in stick representation.

of sbwAFP resulted in a significant loss in activity (30% of wild-type activity) suggesting that the TXT residues are located in the ice-binding face [34]. A similar study was performed using TmAFP, where Thr residues were mutated mainly to Tyr (Thr26→Yyr, Thr38→Yyr, Thr40→Yyr, Thr62→Yyr), with Thr40 also being mutated to Leu or Lys [53]. Generally, a mutation to Tyr caused a 90% loss in TmAFP TH activity. The mutation Thr40→Lys caused the same loss in activity as the mutation to Tyr, while the Thr40→Leu mutation was slightly better tolerated (25% TH activity), which led the authors to suggest that the amount of activity lost may be correlated with the size of the substituted residue [53].

Mutations to leucine were also made to residues Thr48 and Thr66 of sbwAFP, which flank the TXT motif. The alteration caused the TH activity to drop to 70% and 65%, respectively. It is not known whether this indicates that these two residues are peripherally involved in ice binding, or whether the mutation has caused a slight change in the structure of the neighbouring TXT face. A mutation of Thr opposite the TXT face of sbwAFP (Thr86→Leu) had no effect on activity [34]. The control mutation for

TmAFP, Thr43→Yyr (located on the face of the protein opposite to the TXT motif), did result in a minor loss in activity (80% of wild-type TH activity) [53]. This is probably due to the difficulty in folding the protein, rather than suggesting that this face of TmAFP interacts with the ice surface.

It is important to distinguish whether the mutations disrupt the ice-binding interaction by changing the surface properties of the protein, or by altering the structure of the protein. $^1\text{H-NMR}$ and $^1\text{H-}^1\text{H}$ total correlation 2D NMR spectroscopy experiments on Thr7→Leu and Thr36→Leu of sbwAFP did not show any gross changes in structure compared to data from the wild-type protein (S. P. Graether & B. D. Sykes, unpublished data), demonstrating that the structures of these mutants are still highly β -helical. Similarly, NMR data showed that the TmAFP mutant proteins remain mostly well folded [53].

Role of the TXT motif and water in activity

Examination of the crystal structures of the insect AFPs also revealed the presence of an array of water molecules

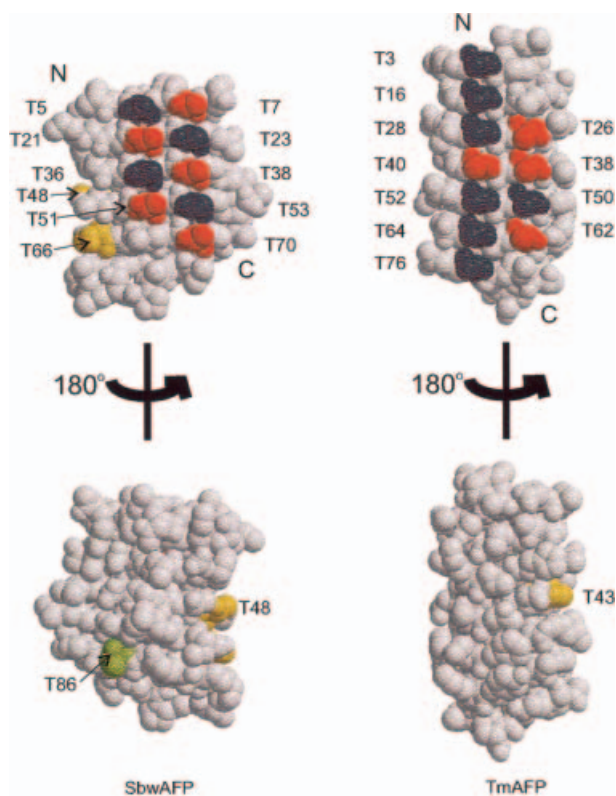


Fig. 5. TXT motif of sbwAFP and TmAFP. CPK representation of sbwAFP (left) and TmAFP (right). Thr residues were individually mutated to Leu (sbwAFP) or to Tyr (TmAFP) and the TH activity of the protein was measured. The top of the panel shows the protein with the TXT face oriented towards the viewer, while the bottom shows the effect of mutations on Thr residues away from the TXT face. Red, 0–10% thermal hysteresis activity relative to wild-type protein; yellow, 50–75% activity; green, 90–100% activity; blue, not mutated.

between the Thr residues in the TXT motif (Fig. 6). For TmAFP, the water molecules bridge the dimer interface in the asymmetric unit. This rank of water molecules, combined with the hydroxyls of the TXT motif, forms a lattice of oxygens with similar spacing as the oxygens in the prism plane ice lattice. Liou *et al.* proposed that this match could form a one-molecule thick layer of water that could be incorporated into an existing ice layer [39]. Molecular dynamics simulations have suggested that after the initial formation of an AFP–ice complex, these water molecules are removed, such that even the transitory formation of a mono-ice layer may be sufficient to aid in TmAFP binding to ice [54].

For sbwAFP, the most conserved waters are found in a trough that flanks the left rank of the TXT face [37]. The water molecules, bonded to carbonyl oxygens, were proposed to extend the size and flatness of the ice-binding face. The rank of water molecules down the middle of the TXT face, as was observed in TmAFP, is not present in any single sbwAFP monomer of the X-ray structure. However, if all the waters from the four molecules in the asymmetric unit are merged onto one structure, we see that the rank of water molecules in the TXT motif are conserved, and that in solution these waters could be found on the ice-binding face

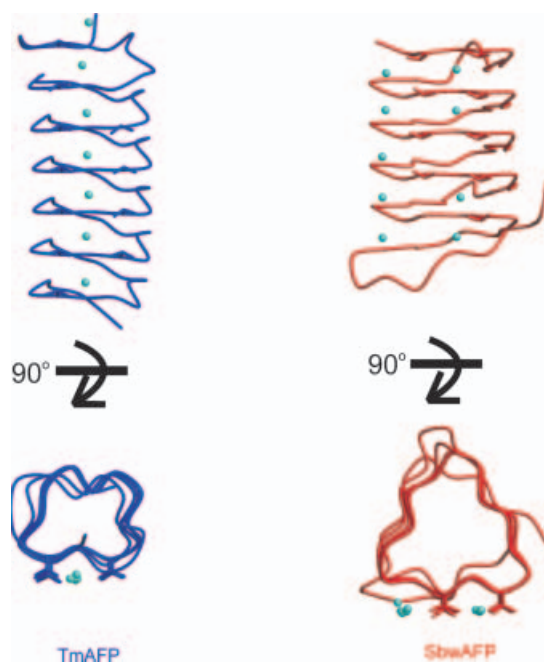


Fig. 6. Bound water molecules extend the ice-binding face of insect AFPs. The position of the water oxygen atoms along the TXT face found in any of the four proteins (sbwAFP, red structure) or two proteins (TmAFP, blue structure) in the asymmetric unit of the crystal are shown as light blue spheres. The Thr side-chains of TXT are shown in stick form while the backbone is shown as a C α trace. The top panel shows a view face-on with the TXT motif, while the bottom panel is a view down the β -helical axis from the N- to the C-terminus.

(Fig. 6). It is possible that the larger array of water molecules in sbwAFP is required to compensate for the greater flexibility of this protein compared to TmAFP, in order to present a better rigid lattice match to the ice surface.

Insect AFP isoforms

In addition to *in vitro* mutations, the comparison of isoform sequences can demonstrate which residues are important for a protein's function and structure. A list of known isoforms may be found in Doucet *et al.* [55] for sbwAFP and in Liou *et al.* [36] for TmAFP. Given the highly repetitive structure of the β -helices, one would expect repetitive sequences. For TmAFP, the isoforms show a 12-residue consensus sequence of TCTXSXXCXXAXT [32,39]. This is not the case for sbwAFP, where only the TXT motif is highly conserved in a single coil. Kajava has suggested the sequence SX(V/I)XG as a pentapeptide repeat for sbwAFP [47], but the motif is only completely conserved in two pentapeptide sequences out of 25.

Imperfect TXT motifs have been observed in almost all sbwAFP and TmAFP isoforms [36,55,56]. Several sbwAFP sequences show that amino acids with large side-chains (e.g. Ile and Arg) can be located in the first Thr rank [56]. Thr ranks are defined such that the first Thr in the sequence Thr-X-Thr is named the first rank. In contrast to the mutagenesis data, this suggests that bulky residues can be accommodated in the first rank without affecting activity. Examination of the crystal structure of sbwAFP did not

show that the bulky TXT residue Ile68 pointing away in order to provide a more complementary surface to ice [57]. Isoform 339, where the first two TXT motifs have a substitution to Arg and Val, respectively, has been expressed [56]. Despite the absence of two Thr residues, isoform 339 has similar activity to isoform 337 (the isoform used in the sbwAFP structural studies). In fact, one gene has been sequenced where all five TXT motifs are perfect [55], but the activity of an expressed protein has not been determined. Based on the propensity of non-Thr residues to be found in the first rank of insect AFPs, Doucet *et al.* hypothesized that ice adsorption may occur via a two-step mechanism [56]. The second rank, which tends to have 100% conservation of Thr, binds first (because it has a more 'complementary' fit to the ice face) followed by the binding of the less conserved Thr rank. This would allow bulky residues to turn away from the ice-binding face, thereby preventing a steric clash between ice and the ice-binding face. It is not clear, however, why naturally present nonthreonine residues are accommodated while similar *in vitro* mutated residues show a large decrease in activity.

Sequencing of cDNAs from both sbwAFP and TmAFP has identified longer isoforms with inserts of 30 or 31 residues for sbwAFP [55,56], and inserts of 12 or 36 residues for TmAFP [36]. These inserts represent the addition of an additional one, two or three β -helical coils compared to the shorter isoforms. In the case of one sbwAFP isoform, named CfAFP-501, a detailed examination of the structure and function was undertaken [57]. An overall match of 66% amino-acid identity was observed, with an insert of 31 residues at position 29 relative to isoform 337. The addition of two coils results in a $\approx 34\%$ increase in area of the TXT region. The first inserted coil is 16 residues long such that a Ser is inserted at the corner opposite the TXT face. This may remove the strain on the β -strand at the TXT motif, ensuring that the face remains flat and provides a good lattice match to the ice surface. An overlap of the two structures can be seen in Fig. 7A, which demonstrates the similarity in structure for the majority of the coils and in the C-terminal caps. An overlap emphasizing the N-terminal cap shows that their structures are in essence identical except for the insert (Fig. 7B).

The TH activity of CfAFP-501 can be as high as three times that of isoform 337. Despite the higher activity than isoform 337, the larger isoform lacks three Thr in the seven TXT motifs (Thr5 \rightarrow Val, Thr37 \rightarrow Ile and Thr52 \rightarrow Val). To test whether the increased activity of CfAFP-501 is due to an increase in the number of TXT motifs, a deletion mutant was created in which the insert from residues 29–59 were removed [57]. The deletion resulted in a protein with slightly lower TH activity than that of the shorter isoform 337 ($\approx 80\%$). These results suggest that it is not only the binding of AFP to two ice faces that result in a higher activity, but that the activity increases with an increase in the number of residues that bind ice (and hence increases the affinity of the protein for ice). The authors also suggest that even longer isoforms, which theoretically may even be better antifreeze proteins, do not exist because they lose their rigidity and hence their ideal lattice match to ice [57]. These results, however, may be contradicted by the work of Marshall *et al.* who examined the partitioning of several wild-type AFPs and mutants between water and ice [58]. Their results

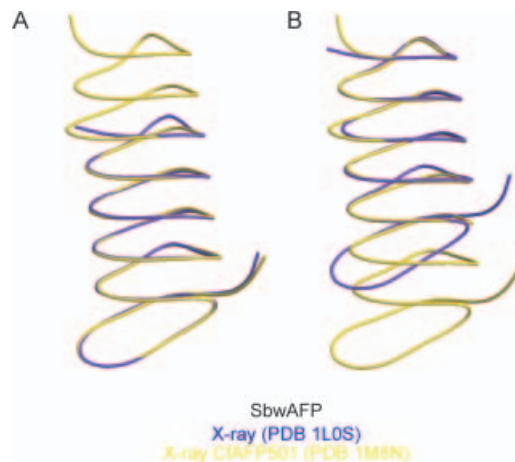


Fig. 7. Comparison of the X-ray structures of sbwAFP isoform 337 with CfAFP-501. The structures are shown as smoothed, C α traces, with the structure and PDB code shown below each panel. (A) Overlap of isoform 337 with the structure of the longer isoform CfAFP-501 using the main chain of residues Thr23 \rightarrow Asn90 in isoform 337 and residues Thr54 \rightarrow Met121 in CfAFP-501. (B) Overlap of isoforms 337 and 501 using the main chain of residues 4–33 in both proteins.

show that despite the > 10 -fold difference in TH activity, fish and insect AFPs partition in equal amounts in ice. The authors claim that they therefore have equal affinity for ice, and that the differences in activity arise from more effective coverage of the ice surface by the insect AFPs. Further experimentation is required to determine what exactly causes the increase in TH activity of CfAFP-501.

Dynamics of insect AFPs

To determine whether changes in temperature cause changes in the structure of the insect AFPs and to further characterize the TXT face of these proteins, the backbone dynamics of TmAFP and sbwAFP were measured at 30 °C and 5 °C [38,40]. Overall, the results suggest that both proteins are rigid, due to the mostly invariant relaxation data and that lowering the temperature increases the protein rigidity. We proposed that these β -helical proteins are rigid most probably because of the extensive network of hydrogen bonds between the coils and the favourable van der Waals interactions between stacked residues [38], a property that has been noted for other β -helical proteins [47]. Additional rigidity in TmAFP arises from the eight disulphide bridges in the core of the protein.

Two studies by Daley & Sykes examined the conformation of the Thr side-chains in TmAFP at 30 °C and 5 °C [59,60]. In their first series of experiments [59], NMR data were analyzed to examine the preference of Thr residues for particular rotameric states. The results showed that TXT threonines had a preference for $\chi_1 = -60^\circ$ at 30 °C, with an increase for this preference as the temperature was lowered to 5 °C. In contrast, Thr residues away from the ice-binding face showed no preference for χ_1 . These experiments, however, are not able to characterize the rates of transfer between rotameric states or the amount of librational

motions. In the second study, no significant rotation about the χ_1 dihedral angle was observed, and analysis of the C_β atoms of the TXT threonines found them to be as motionally rigid as the backbone [60]. Taken together, these experiments show that the TXT side-chains are highly rigid. This suggests that the ice-binding site of TmAFP is preformed in solution even at elevated temperatures, which reduces the entropic barrier that would be associated with the re-arrangement of the TXT Thr side-chains before binding to the ice surface [40,59,60].

For sbwAFP, analysis of the NMR relaxation data revealed that the protein forms oligomers [38]. Diluting the protein showed the interaction to be concentration dependent. An estimation of the dimer affinity suggests that the dissociation constant is in the millimolar range, and most probably not relevant to antifreeze activity *in vivo*. The oligomers may represent the repetitive face of sbwAFP binding to the complementary face on another AFP molecule. This proposal is supported by the structure of the asymmetric unit in the sbwAFP crystal. This unit contains two dimers, where the interface occurs near the TXT face of the protein with the termini in a parallel orientation (i.e. the termini are N to N and C to C). A dimer was also observed in the asymmetric unit of the TmAFP crystal structure. There is no evidence of TmAFP oligomerization in the NMR [40] or ultracentrifugation data [43]. Taken together, the data suggest that the oligomerization is observed simply because of the complimentary nature of the repetitive structures and the high concentration of protein used in NMR and X-ray crystallography, and does not likely represent an interaction relevant to the function of these antifreeze proteins.

Comparison of sbwAFP to TmAFP

Although sbwAFP and TmAFP both consist of β -helical folds, their backbone atoms do not have identical geometries. Specifically, the size of the coils and the helical handedness are different, with the spruce budworm protein consisting of 15-residue coils with a left-handed fold and the *Tenebrio molitor* protein consisting of 12-residue coils with a right-handed fold (compare the structures in Fig. 2). The difference in handedness is somewhat analogous to studies performed with L- and D-amino acid type I AFP [61,62]. In these experiments, both type I AFPs were shown to be equally effective inhibitors of ice growth, but bound in mirror-image directions along specific ice planes.

In both sbwAFP and TmAFP, the TXT motif is highly conserved and has been shown by mutagenesis to be involved in the ice-binding interaction [34,53]. Based on this sequence conservation, we overlapped sbwAFP and TmAFP using only the C_α atoms of the threonines in the TXT motif (Fig. 8A). Given the different handedness, the proteins align with the termini orientations opposite to one another, yet the Thr side chain atoms overlap completely. An alignment of a single coil from each protein is shown in Fig. 8B. TmAFP, with coils that are three residues shorter than that of sbwAFP, has a much tighter coil path. Another effect of the tighter coils is that TmAFP has one and a half extra coils along the TXT face (Fig. 8A). This gives TmAFP one and a half additional TXT motifs along the ice-binding face, though the C-terminal motif contains an imperfect Ala-Cys-Thr sequence and only two Thr in the first two coils. Nevertheless, both proteins present an essentially identical ice-binding face that is considerably better at

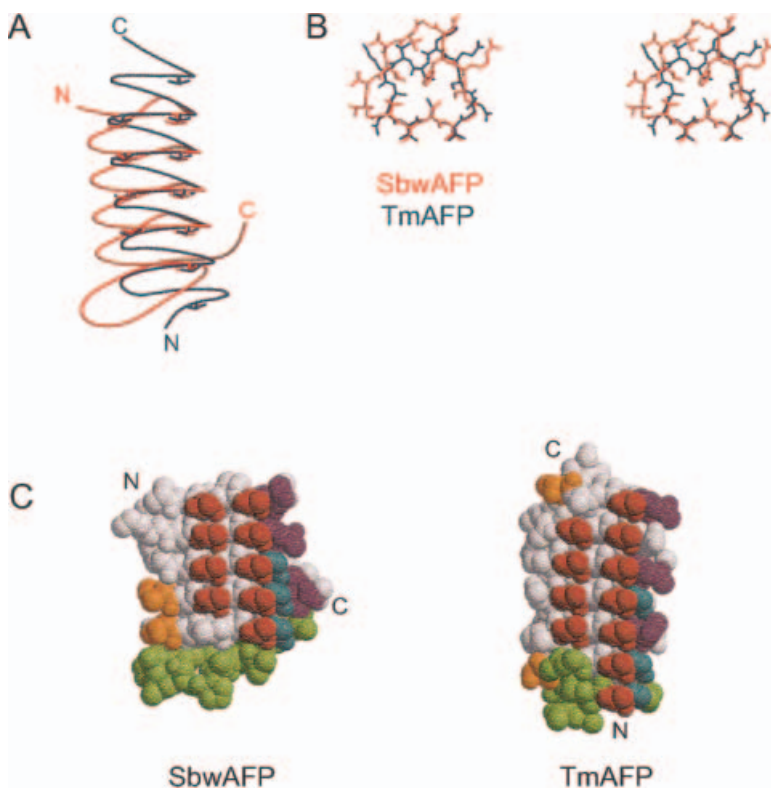


Fig. 8. A comparison of sbwAFP and TmAFP structures.

(A) An overlap of smoothed C_α traces obtained by overlapping the C_α atoms of the Thr residues of the TXT motifs. The Thr side-chains of the TXT face are shown in a stick representation. Note that the orientations of the N- and C-termini of the proteins are inverted with respect to one another.

(B) Stereo view of a cross-section of an overlapped coil of the sbwAFP (residues Gly34 to Thr49, red) and TmAFP (residues Asn29 to Gly41, blue) shown in stick representation. The loops are overlapped using the same atoms as in (A).

(C) CPK representation of sbwAFP (left) and TmAFP (right) colored to show the similar organization of different structure and sequence elements. As in (A), the termini of the proteins are oriented opposite to one another. Red, TXT face; orange, flanking Thr residues; blue, Gly residues; purple, Asn residues; green, C- (sbwAFP) or N-terminal (TmAFP) cap.

inhibiting ice growth than the previously characterized fish AFPs. Ice-etching studies with sbwAFP suggest that the protein binds both basal and prism planes of ice [34]. Given the identical arrangement of the ice-binding face of TmAFP, one would expect that it too could bind basal and prism planes. However, conclusive ice-etching data is not yet published for TmAFP. Ice morphology studies have revealed a potential difference in ice plane preference: sbwAFP ice crystals are approximately hexagonal in shape, while TmAFP ice crystals resemble teardrops [32].

Further examination of the structure and sequence of sbwAFP and TmAFP reveal other similarities (Fig. 8C). The panel shows the similarity of the TXT face again, and also reveals the presence of two Thr flanking one side of the TXT face (Thr49 and Thr66 in sbwAFP; Thr12 and Thr73 in TmAFP). Mutagenesis of Thr66→Leu caused a reduction in TH activity, which suggests that these threonines may be peripherally involved in the ice-binding interaction. The panel also demonstrates that the first rank of Thr in the TXT motifs is less conserved than the second rank. This observation has also been seen in the sbwAFP isoform studies noted above. This substitution pattern is not as obvious for TmAFP, where Ala is found in the first position of the C-terminal TXT motif. Otherwise, there is very little isoform substitution of TXT residues, due to the tight coil structure. The conservation of Gly and Asn residues is seen on the right side of each structure in Fig. 8C. The Gly residues probably represent the presence of small amino acids at corners of the β -helices in order to allow for the tight turns. Stacks of Asn residues have also been found in other β -helical proteins. These Asn residues, however, are located inside the core of the protein and make hydrogen bonds to the backbone carbonyl oxygens and amides; in the insect AFPs, the side-chains face into solution and do not make any such bonds. Recently, conserved, outward pointing Asn residues have been shown to be important in the carrot AFP TH activity [63]. It would be interesting to determine whether the insect AFPs Asn residues are also somehow involved in ice binding.

Both sbwAFP and TmAFP have a capping structure at one terminus. In the case of sbwAFP, the cap is at the C-terminus while for TmAFP is at the N-terminus. This pattern agrees with that of other β -helical proteins, where left-handed hexapeptide repeat β -helices caps are at the C-terminus, while right-handed β -helices tend to have a cap at the N-terminus (Fig. 4). The exact role of the cap structure has not been determined, but it is possible that the caps help to determine the handedness of the proteins, or may prevent the unfolding of the protein at cold temperatures.

The β -helix as an AFP structural motif?

The sbwAFP and TmAFP structures represent the first AFPs characterized to have a β -helical fold. Recent modelling studies had suggested that the *Dendroides canadensis* AFP (DAFP) [12], *Lolium perenne* (ryegrass) AFP (LpAFP) [64], and *Daucus carota* (carrot) AFP (DcAFP) [63] may all possess β -helical folds (Fig. 9). The conserved insect AFP TXT motif is not necessarily present in these modelled AFPs. In the *Lolium perenne* protein, several imperfect TXT motifs (i.e. a mixture of Thr, Ser and Val

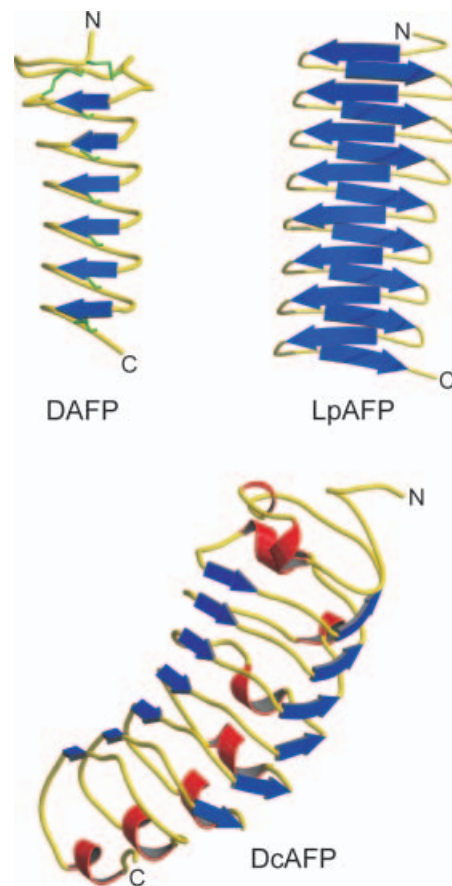


Fig. 9. β -Helical models of several antifreeze proteins. The color scheme in the ribbon representation is the same as that of Fig. 1. Figures are shown with N-termini at the top and C-termini near the bottom of the figure. The *Lolium perenne* (LpAFP) model is from PDB deposition (1I3B) [64], while the DAFP and DcAFP models are based on sequence alignments from the published models [12,63]. The putative ice-binding face of each model is oriented towards the viewer.

residues) were found on two faces of the protein, which, in combination with its superior ice-recrystallization inhibition, lead to the hypothesis that the protein may have two ice-binding faces [64]. For DcAFP, the conserved Asn side-chains were shown to be important in ice binding [63]. These structures and models lend further support to the proposal that the β -helical fold is an ideal scaffold for making a molecular match to the lattice of water molecules arrayed in ice. The ideal fit may arise from the interstrand spacing of the β -sheets (4.75 Å), which is a close match to the spacing of oxygen in ice on the prism plane (4.5 Å) [34].

Ice nucleation proteins (INPs), which represent the antithesis of AFPs in that INPs promote the formation of ice [65–67], have been suggested to form β -helices [68]. The INP sequence contains 61 16-residue repeats (AGYG STXTAXXXSXLX) flanked by nonrepetitive N- and C-terminal regions [69]. Note that INPs, like the insect AFPs, also contain a TXT motif. Graether & Jia proposed that the size of the ice-binding face of sbwAFP is $\approx 1/4000\times$ the size of an ice embryo required to promote ice growth at -2°C , whereas the INP oligomer is approximately half the required size [68]. Therefore, the ability to inhibit ice growth,

as occurs with insect AFPs, vs. the ability to promote growth, is based on the size of the protein. Although both proteins may be able to form an ice-like arrangement of water on the protein surface, only INPs are large enough to support continued growth.

Conclusion

Analysis of the structure and examination of the ice-binding behaviour and point mutants of sbwAFP and TmAFP provides an explanation for their hyperactivity compared to the previously characterized fish AFPs. The β -helix fold presents a rigid array of TXT residues that, along with bound water molecules, is able to mimic the ice lattice of the prism and basal planes, and is thus able to provide more effective coverage of the ice surface compared to the fish AFPs. Despite having been characterized five years ago, no other β -helical protein with the same number of residues per coil has had its structure determined. Sequence identity searches have not revealed any other matches, suggesting that these particular β -helical folds may remain rare for the near future. Nevertheless, the sequencing of two new AFPs (from ryegrass and carrots) strongly suggests that the β -helix may be a new structural motif for AFPs. This contrasts with fish AFPs, where four different folds have been described [12].

Even so, a considerable number of questions remain before we can solve the interaction at the atomic level and understand the role of the threonine side chains in ice binding. The contradiction between the higher activity demonstrated by the longer insert AFP isoforms vs. the lack of change in the partition coefficient of TmAFP compared to fish AFPs suggests that ice-binding cannot be thought of as a simple interaction, but must begin to include principles that do not apply to conventional protein–ligand interactions. These include such issues as simulating the presence of the AFPs in a ‘sluggish-water’ layer [70] or the possibility that the protein modifies the ice surface after binding, such that further growth is inhibited, or that more than one face of an AFP can simultaneously interact with the ice surface. Some answers may come from more studies on the structure of the protein in ice [50], or from studies of the surface chemistry properties of ice itself.

Acknowledgements

We thank Drs Peter L. Davies and Zongchao Jia for discussions and financial support of the structural studies. We also thank Dr Jin-Fa Wang for providing the coordinates to the *Daucus carota* antifreeze protein model. This work is supported by grants from the Canadian Institutes of Health Research (CIHR), the Government of Canada’s Network of Centres of Excellence program (supported by CIHR and Natural Science and Engineering Research Council of Canada through the Protein Engineering Network of Centres of Excellence, Inc.; B. D. S). S. P. G. is the recipient of a CIHR Fellowship and an Alberta Heritage Fund for Medical Research Fellowship.

References

1. Storey, K.B. & Storey, J.M. (1991) Biochemistry of cryoprotectants. In *Insects at Low Temperatures* (Lee, R.E. & Denlinger, D., eds), pp. 64–93. Chapman & Hall, New York, USA.
2. Fletcher, G.L., Hew, C.L. & Davies, P.L. (2001) Antifreeze Proteins of Teleost Fishes. *Annu. Rev. Physiol.* **63**, 359–390.
3. Breton, G., Danyluk, J., Ouellet, F. & Sarhan, F. (2000) Biotechnological applications of plant freezing associated proteins. *Biotechnol. Annu. Rev.* **6**, 59–101.
4. Gilbert, J.A., Hill, P.J., Dodd, C.E.R. & Laybourn-Parry, J. (2004) Demonstration of antifreeze protein activity in Antarctic lake bacteria. *Microbiology* **150**, 171–180.
5. Hoshino, T., Kiriaki, M., Ohgiya, S., Fujiwara, M., Kondo, H., Nishimiya, Y., Yumoto, I. & Tsuda, S. (2003) Antifreeze proteins from snow mold fungi. *Can. J. Bot.-Revue Can. Bot.* **81**, 1175–1181.
6. Duman, J.G. (2001) Antifreeze and ice nucleator proteins in terrestrial arthropods. *Annu. Rev. Physiol.* **63**, 327–357.
7. Raymond, J.A. & DeVries, A.L. (1977) Adsorption inhibition as a mechanism of freezing resistance in polar fishes. *Proc. Natl Acad. Sci. USA* **74**, 2589–2593.
8. Wilson, P.W. & Leader, J.P. (1995) Stabilization of supercooled fluids by thermal hysteresis proteins. *Biophys. J.* **68**, 2098–2107.
9. Davies, P.L. & Sykes, B.D. (1997) Antifreeze proteins. *Curr. Opin. Struct. Biol.* **7**, 828–834.
10. Ewart, K.V., Lin, Q. & Hew, C.L. (1999) Structure, function and evolution of antifreeze proteins. *Cell Mol. Life Sci.* **55**, 271–283.
11. Yeh, Y. & Feeney, R.E. (1996) Antifreeze proteins: Structures and mechanisms of function. *Chem. Rev.* **96**, 601–617.
12. Jia, Z. & Davies, P.L. (2002) Antifreeze proteins: an unusual receptor–ligand interaction. *Trends Biochem. Sci.* **27**, 101–106.
13. Sönnichsen, F.D., Davies, P.L. & Sykes, B.D. (1998) NMR structural studies on antifreeze proteins. *Biochem. Cell Biol.* **76**, 284–293.
14. Tachibana, Y., Fletcher, G.L., Fujitani, N., Tsuda, S., Monde, K. & Nishimura, S.I. (2004) Antifreeze glycoproteins: elucidation of the structural motifs that are essential for antifreeze activity. *Angew. Chem. Int.*, **43**, 856–862.
15. Ben, R.N. (2001) Antifreeze glycoproteins – preventing the growth of ice. *ChemBiochemistry* **2**, 161–166.
16. Harding, M.M., Anderberg, P.I. & Haymet, A.D. (2003) ‘Antifreeze’ glycoproteins from polar fish. *Eur. J. Biochem.* **270**, 1381–1392.
17. Sicheri, F. & Yang, D.S. (1995) Ice-binding structure and mechanism of an antifreeze protein from winter flounder. *Nature* **375**, 427–431.
18. Yang, D.S., Sax, M., Chakrabarty, A. & Hew, C.L. (1988) Crystal structure of an antifreeze polypeptide and its mechanistic implications. *Nature* **333**, 232–237.
19. DeVries, A.L. & Lin, Y. (1977) Structure of a peptide antifreeze and mechanism of adsorption to ice. *Biochim. Biophys. Acta* **495**, 388–392.
20. Knight, C.A., Cheng, C.C. & DeVries, A.L. (1991) Adsorption of alpha-helical antifreeze peptides on specific ice crystal surface planes. *Biophys. J.* **59**, 409–418.
21. Wen, D. & Laursen, R.A. (1992) A model for binding of an antifreeze polypeptide to ice. *Biophys. J.* **63**, 1659–1662.
22. Chao, H., Houston, M.E., Hodges, R.S., Kay, C.M., Sykes, B.D., Loewen, M.C., Davies, P.L. & Sönnichsen, F.D. (1997) A diminished role for hydrogen bonds in antifreeze protein binding to ice. *Biochemistry* **36**, 14652–14660.
23. Haymet, A.D., Ward, L.G., Harding, M.M. & Knight, C.A. (1998) Valine substituted winter flounder ‘antifreeze’: preservation of ice growth hysteresis. *FEBS Lett.* **430**, 301–306.
24. Zhang, W. & Laursen, R.A. (1998) Structure-function relationships in a type I antifreeze polypeptide. The role of threonine methyl and hydroxyl groups in antifreeze activity. *J. Biol. Chem.* **273**, 34806–34812.

25. Baardsnes, J., Kondejewski, L.H., Hodges, R.S., Chao, H., Kay, C. & Davies, P.L. (1999) New ice-binding face for type I antifreeze protein. *FEBS Lett.* **463**, 87–91.
26. Gronwald, W., Loewen, M.C., Lix, B., Daugulis, A.J., Sönnichsen, F.D., Davies, P.L. & Sykes, B.D. (1998) The solution structure of type II antifreeze protein reveals a new member of the lectin family. *Biochemistry* **37**, 4712–4721.
27. Sönnichsen, F.D., DeLuca, C.I., Davies, P.L. & Sykes, B.D. (1996) Refined solution structure of type III antifreeze protein: hydrophobic groups may be involved in the energetics of the protein–ice interaction. *Structure* **4**, 1325–1337.
28. Jia, Z., DeLuca, C.I., Chao, H. & Davies, P.L. (1996) Structural basis for the binding of a globular antifreeze protein to ice. *Nature* **384**, 285–288.
29. Yang, D.S., Hon, W.C., Bubanko, S., Xue, Y., Seetharaman, J., Hew, C.L. & Sicheri, F. (1998) Identification of the ice-binding surface on a type III antifreeze protein with a ‘flatness function’ algorithm. *Biophys. J.* **74**, 2142–2151.
30. Antson, A.A., Smith, D.J., Roper, D.I., Lewis, S., Caves, L.S., Verma, C.S., Buckley, S.L., Lillford, P.J. & Hubbard, R.E. (2001) Understanding the mechanism of ice binding by type III antifreeze proteins. *J. Mol. Biol.* **305**, 875–889.
31. Tyshenko, M.G., Doucet, D., Davies, P.L. & Walker, V.K. (1997) The antifreeze potential of the spruce budworm thermal hysteresis protein. *Nat. Biotechnol.* **15**, 887–890.
32. Graham, L.A., Liou, Y.C., Walker, V.K. & Davies, P.L. (1997) Hyperactive antifreeze protein from beetles. *Nature* **388**, 727–728.
33. Andorfer, C.A. & Duman, J.G. (2000) Isolation and characterization of cDNA clones encoding antifreeze proteins of the pyrochroid beetle *Dendroides canadensis*. *J. Insect Physiol.* **46**, 365–372.
34. Graether, S.P., Kuiper, M.J., Gagné, S.M., Walker, V.K., Jia, Z., Sykes, B.D. & Davies, P.L. (2000) Beta-helix structure and ice-binding properties of a hyperactive antifreeze protein from an insect. *Nature* **406**, 325–328.
35. Wilson, P., Gould, M. & DeVries, A. (2002) Hexagonal shaped ice spicules in frozen antifreeze protein solutions. *Cryobiology* **44**, 240.
36. Liou, Y.C., Thibault, P., Walker, V.K., Davies, P.L. & Graham, L.A. (1999) A complex family of highly heterogeneous and internally repetitive hyperactive antifreeze proteins from the beetle *Tenebrio molitor*. *Biochemistry* **38**, 11415–11424.
37. Leinala, E.K., Davies, P.L. & Jia, Z. (2002) Crystal Structure of beta-Helical Antifreeze Protein Points to a General Ice Binding Model. *Structure* **10**, 619–627.
38. Graether, S.P., Gagné, S.M., Spyropoulos, L., Jia, Z., Davies, P.L. & Sykes, B.D. (2003) Spruce budworm antifreeze protein: changes in structure and dynamics at low temperature. *J. Mol. Biol.* **327**, 1155–1168.
39. Liou, Y.C., Tocilj, A., Davies, P.L. & Jia, Z. (2000) Mimicry of ice structure by surface hydroxyls and water of a beta-helix antifreeze protein. *Nature* **406**, 322–324.
40. Daley, M.E., Spyropoulos, L., Jia, Z., Davies, P.L. & Sykes, B.D. (2002) Structure and dynamics of a beta-helical antifreeze protein. *Biochemistry* **41**, 5515–5525.
41. Jenkins, J. & Pickersgill, R. (2001) The architecture of parallel β-helices and related folds. *Prog. Biophys. Mol. Biol.* **77**, 111–175.
42. Gauthier, S.Y., Kay, C.M., Sykes, B.D., Walker, V.K. & Davies, P.L. (1998) Disulfide bond mapping and structural characterization of spruce budworm antifreeze protein. *Eur. J. Biochem.* **258**, 445–453.
43. Liou, Y.C., Daley, M.E., Graham, L.A., Kay, C.M., Walker, V.K., Sykes, B.D. & Davies, P.L. (2000) Folding and structural characterization of highly disulfide-bonded beetle antifreeze protein produced in bacteria. *Protein Expr. Purif.* **19**, 148–157.
44. Yoder, M.D., Keen, N.T. & Jurnak, F. (1993) New domain motif: the structure of pectate lyase C, a secreted plant virulence factor. *Science* **260**, 1503–1507.
45. Raetz, C.R. & Roderick, S.L. (1995) A left-handed parallel beta helix in the structure of UDP-N-acetylglucosamine acyltransferase. *Science* **270**, 997–1000.
46. Richardson, J.S. (1976) Handedness of crossover connections in beta sheets. *Proc. Natl Acad. Sci. USA* **73**, 2619–2623.
47. Kobe, B. & Kajava, A.V. (2000) When protein folding is simplified to protein coiling: the continuum of solenoid protein structures. *Trends Biochem. Sci.* **25**, 509–515.
48. Lazo, N.D. & Downing, D.T. (1997) Beta-helical fibrils from a model peptide. *Biochem. Biophys. Res. Commun.* **235**, 675–679.
49. Lazo, N.D. & Downing, D.T. (1998) Amyloid fibrils may be assembled from beta-helical protofibrils. *Biochemistry* **37**, 1731–1735.
50. Graether, S.P., Slupsky, C.M. & Sykes, B.D. (2003) Freezing of a fish antifreeze protein results in amyloid fibril formation. *Biophys. J.* **84**, 552–557.
51. Shindyalov, I.N. & Bourne, P.E. (1998) Protein structure alignment by incremental combinatorial extension (CE) of the optimal path. *Protein Eng.* **11**, 739–747.
52. Duman, J.G., Verleye, D. & Li, N. (2002) Site-specific forms of antifreeze protein in the beetle *Dendroides canadensis*. *J. Comp. Physiol. [B]* **172**, 547–552.
53. Marshall, C., Daley, M., Graham, L., Sykes, B.D. & Davies, P. (2002) Identification of the ice-binding face of antifreeze protein from *Tenebrio molitor*. *FEBS Lett.* **529**, 261.
54. Yang, Z., Zhou, Y., Liu, K., Cheng, Y., Liu, R., Chen, G. & Jia, Z. (2003) Computational study on the function of water within a beta-helix antifreeze protein dimer and in the process of ice-protein binding. *Biophys. J.* **85**, 2599–2605.
55. Doucet, D., Tyshenko, M.G., Davies, P.L. & Walker, V.K. (2002) A family of expressed antifreeze protein genes from the moth, *Choristoneura fumiferana*. *Eur. J. Biochem.* **269**, 38–46.
56. Doucet, D., Tyshenko, M.G., Kuiper, M.J., Graether, S.P., Sykes, B.D., Daugulis, A.J., Davies, P.L. & Walker, V.K. (2000) Structure-function relationships in spruce budworm antifreeze protein revealed by isoform diversity. *Eur. J. Biochem.* **267**, 6082–6088.
57. Leinala, E.K., Davies, P.L., Doucet, D., Tyshenko, M.G., Walker, V.K. & Jia, Z. (2002) A beta-helical antifreeze protein isoform with increased activity: structural and functional insights. *J. Biol. Chem.* **277**, 33349–33352.
58. Marshall, C.B., Tomczak, M.M., Gauthier, S.Y., Kuiper, M.J., Lankin, C., Walker, V.K. & Davies, P.L. (2004) Partitioning of fish and insect antifreeze proteins into ice suggests they bind with comparable affinity. *Biochemistry* **43**, 148–154.
59. Daley, M.E. & Sykes, B.D. (2003) The role of side chain conformational flexibility in surface recognition by *Tenebrio molitor* antifreeze protein. *Protein Sci.* **12**, 1323–1331.
60. Daley, M.E. & Sykes, B.D. (2004) Characterization of threonine side chain dynamics in an antifreeze protein using natural abundance (¹³C) NMR spectroscopy. *J. Biomol. NMR* **29**, 139–150.
61. Wen, D. & Laursen, R.A. (1993) A D-antifreeze polypeptide displays the same activity as its natural L-enantiomer. *FEBS Lett.* **317**, 31–34.
62. Laursen, R.A., Wen, D.Y. & Knight, C.A. (1994) Enantioselective adsorption of the D-forms and L-forms of an alpha-helical antifreeze polypeptide to the (20(-),1) planes of ice. *J. Am. Chem. Soc.* **116**, 12057–12058.
63. Zhang, D.Q., Liu, B., Feng, D.R., He, Y.M., Wang, S.Q., Wang, H.B. & Wang, J.F. (2004) Significance of conservative asparagine residues in the thermal hysteresis activity of carrot antifreeze protein. *Biochem. J.* **377**, 589–595.

64. Kuiper, M.J., Davies, P.L. & Walker, V.K. (2001) A theoretical model of a plant antifreeze protein from *Lolium perenne*. *Biophys. J.* **81**, 3560–3565.
65. Warren, G. & Wolber, P. (1991) Molecular aspects of microbial ice nucleation. *Mol. Microbiol.* **5**, 239–243.
66. Gurian-Sherman, D. & Lindow, S.E. (1993) Bacterial ice nucleation: significance and molecular basis. *FASEB J.* **7**, 1338–1343.
67. Hew, C.L. & Yang, D.S. (1992) Protein interaction with ice. *Eur. J. Biochem.* **203**, 33–42.
68. Graether, S.P. & Jia, Z. (2001) Modeling *Pseudomonas syringae* ice-nucleation protein as a β -helical protein. *Biophys. J.* **80**, 1169–1173.
69. Wolber, P. & Warren, G. (1989) Bacterial ice-nucleation proteins. *Trends Biochem. Sci.* **14**, 179–182.
70. Hayward, J.A. & Haymet, A.D.J. (2002) The ice/water interface: orientational order parameters for the basal, prism, {2021}, and {2110} interfaces of ice Ih. *Phys Chem. Chem. Physics* **4**, 3712–3719.
71. Breiter, D.R., Kanost, M.R., Benning, M.M., Wesenberg, G., Law, J.H., Wells, M.A., Rayment, I. & Holden, H.M. (1991) Molecular structure of an apolipoprotein determined at 2.5-Å resolution. *Biochemistry* **30**, 603–608.
72. Kraulis, P.J. (1991) MOLSCRIPT – A program to produce both detailed and schematic plots of protein structures. *J. Appl. Crystallogr.* **24**, 946–950.
73. Merritt, E.A. & Bacon, D.J. (1997) Raster3D: Photorealistic molecular graphics. *Macromolecular Crystallogr., Part B* **277**, 505–524.